

# Assessment and Management of Existing Bridges Following the Innovative Italian Guidelines: A Pilot Study

Fabrizio Gara<sup>1</sup>; Sandro Carbonari<sup>2</sup>; Vanni Nicoletti<sup>3,\*</sup>; Riccardo Martini<sup>4</sup>; Anna Brunetti<sup>5</sup>; Andrea Torsani<sup>6</sup>; and Andrea Dall'Asta<sup>7</sup>

Submitted: 23 November 2024 Accepted: 03 December 2024 Publication date: 10 January 2025

DOI: 10.70465/ber.v2i1.19

**Abstract:** In 2022, the Italian Government introduced innovative regulations for evaluating and monitoring existing bridges and viaducts, tackling issues related to risk classification, safety assessment, and monitoring. These regulations employ a multilevel approach for bridge inspections, safety assessments, and monitoring procedures. The guidelines have garnered international acclaim for their forward-thinking approach. This paper proposes a comprehensive study concerning the whole process proposed in the new Italian guidelines, using a case study constituted by two prestressed RC box-girder half-joint span bridges that exhibited signs of aging several years ago. The paper deeply addresses all phases of the existing bridge safety assessment and management discussed in the guidelines from both a scientific and practical standpoint, in collaboration with the national agency for road administration. It starts with visual inspections conducted to support the bridge safety assessments and concludes with the experimental testing and structural monitoring of bridges. The objective of this paper is to present advanced procedures for the classification, evaluation, and management of existing bridges to be adopted by road administrators, which may inspire international readers to upgrade the codes of their own countries.

**Author keywords:** Italian guidelines; existing bridges; bridges multi-risk assessment; post-tensioned concrete bridges; box-girder bridges; half-joints; bridge visual inspections; safety verifications; bridge testing and monitoring

## Introduction

Bridges play a crucial role in transportation systems globally. However, insufficient maintenance and supervision over time resulted in the gradual degradation of their structural

integrity, jeopardizing their safe use despite their significance to the social and economic welfare of communities.<sup>1,2</sup> Collapses occurring worldwide have highlighted the vulnerability of bridges to both human and natural factors, such as overloading, design flaws, inadequate inspections, and poor maintenance.<sup>3-6</sup> For these reasons, many authorities worldwide are now discussing the adoption of regulations or standards to be used for managing the infrastructural asset,<sup>7</sup> taking inspiration from those already available. For instance, the American Federal Highway Administration released in 2022 the adjourned version of the National Bridge Inspection Standards (NBIS) dealing with bridge inspection procedures and intervals based on a risk-based approach. In the UK, the Highways England issued the CS 450, providing technical guidance for the routine and special inspection of bridges, while in Japan, the Japan Road Association established a comprehensive framework for the routine inspection, maintenance, and management of bridges (the Japanese Bridge Inspection Standards). The latter also emphasizes advanced inspection technologies such as sensors and real-time monitoring to assess the health status of bridges due to the country's high vulnerability to natural disasters. The Australian standard (AS 5100) contains provisions related to bridge inspection, outlining maintenance and rehabilitation guidelines for bridges, including inspection procedures. The Canadian Highway Bridge Design Code (CSA S6) includes guidelines on bridge

\*Corresponding Author: Vanni Nicoletti.

Email: v.nicoletti@univpm.it

<sup>1</sup>Full Professor, Department of Construction, Civil Engineering and Architecture (DICEA), Università Politecnica delle Marche, Via Breccia Bianche 12, 60131, Ancona, Italy

<sup>2</sup>Associate Professor, Department of Construction, Civil Engineering and Architecture (DICEA), Università Politecnica delle Marche, Via Breccia Bianche 12, 60131, Ancona, Italy

<sup>3</sup>Assistant Professor, Department of Construction, Civil Engineering and Architecture (DICEA), Università Politecnica delle Marche, Via Breccia Bianche 12, 60131, Ancona, Italy

<sup>4</sup>Post-doc Researcher, Department of Construction, Civil Engineering and Architecture (DICEA), Università Politecnica delle Marche, Via Breccia Bianche 12, 60131, Ancona, Italy

<sup>5</sup>PhD Student, Department of Construction, Civil Engineering and Architecture (DICEA), Università Politecnica delle Marche, Via Breccia Bianche 12, 60131, Ancona, Italy

<sup>6</sup>Head of Infrastructure Inspection Department, ANAS S.p.a., Marche Region Department, Via Isonzo 15, 60124, Ancona, Italy

<sup>7</sup>Full Professor, School of Science and Technology (STT), University of Camerino, Via Gentile da Varano III, 26, 62032, Camerino, Italy

Discussion period open till six months from the publication date. Please submit separate discussion for each individual paper. This paper is a part of the Vol. 1 of the International Journal of Bridge Engineering, Management and Research (© BER), ISSN 3065-0569.

inspection, evaluation, and maintenance. It mandates periodic inspections and includes specific criteria for safety evaluations. The Chinese Bridge Inspection Code (JTG/T J21) is part of the technical specifications for highway bridges in China, providing detailed procedures for regular inspections, defect identification, and condition assessment. In Europe, the Eurocodes primarily provide bridge structural design guidelines, although certain parts (especially EN 1991-2 and EN 1993-2) address the durability and inspection of bridges under different load conditions. However, these documents adopted by several countries around the world address the subject of road infrastructure safety management in a partial and multifaceted manner, and none of them comprehensively deals with management, from the inspection phase to safety verifications.

Because of the lack of detailed and comprehensive regulations in Europe (and worldwide), the Italian Government recently decided to adopt specific regulations for the multi-risk assessment of existing bridges and viaducts to address issues related to the classification of risks, safety assessment and monitoring. These regulations were first published by the Italian Higher Council of Public Works as “Guidelines 2020”,<sup>8</sup> and later updated in 2022<sup>9</sup> when operative instructions were also published by ANSFISA.<sup>10</sup> The latest version of these guidelines is hereinafter referred to as “Guidelines 2022”. The regulations address the multi-risk evaluation and classification for bridges and viaducts through a multilevel approach, consisting of the census and geo-localization of the structure, the visual inspections, the risk classification (through the determination of a Class of Attention–CoA–ranging from Low, Medium-Low, Medium, Medium-High, and High), and the safety assessment and monitoring procedures.<sup>11,12</sup> Importantly, this approach considers various types of risk arising from structural vulnerabilities and the surrounding environment, encompassing structural and foundational risks due to service loads,<sup>13,14</sup> seismic risk, landslide risk, and hydraulic risk, all of which are comprehensively evaluated according to hazard, vulnerability, and exposure. For all these reasons, the new Guidelines 2022 are considered a very cutting-edge document that gained attention in many parts of the world.

Although only recently published, a fair number of papers can already be found in the literature dealing with Guidelines 2022. Some works describe the document content<sup>15,16</sup> and, in some cases, propose comparisons with other condition rating systems around the world.<sup>17,18</sup> Other works discuss statistical analyses of visual inspection results trying to correlate the detected defects and the bridge typology.<sup>19–23</sup> Many of these works show examples of applications in real bridges, mainly focusing on the prestressed concrete ones.<sup>24–28</sup> However, all these works treat the first parts of the Guidelines 2022, namely the visual inspections, risk classifications, and, sometimes, the safety assessment verifications. To the best of the authors’ knowledge, only one paper is available in the scientific literature also discussing the experimental tests for the characterization of the structural (and dynamic) behavior and the monitoring of existing bridges, as proposed in part III, section 7.3, of the Guidelines 2022.<sup>29</sup> However, this work is focused on a footbridge and does not address

the Structural Health Monitoring (SHM) task. Thus, there are no comprehensive applications in the literature yet that provide guidance of interest to practitioners and researchers.

This paper presents a pilot study of the new Italian guidelines from both a scientific and practical standpoint focusing on prestressed concrete bridges. The study delves into all stages of the existing bridge safety assessment and management as outlined in these innovative guidelines. Moreover, differently from articles already available in the literature, the experimental testing and structural monitoring of bridges following the prescriptions of the last part of the Guidelines 2022 (Part III), are also addressed in this work. The main objective of the paper is to provide advanced procedures for the classification, evaluation, and management of existing bridges in line with the philosophy of the innovative Guidelines 2022, offering the first comprehensive discussion on their application in the scientific literature. In this work, a detailed description of the guidelines content is not reported, and only the general philosophy is discussed. Indeed, more importance has been given to showing a complete application of this document’s prescriptions. Readers interested in delving deeper into the Guidelines 2022 content may refer to the works of Santarsiero et al.<sup>15</sup> and Natali et al.<sup>16</sup>

From a practical standpoint, the paper takes advantage of the long expertise of the Italian Autonomous National Agency for Road Administration (ANAS S.p.A.). To this end, two existing post-tensioned Reinforced Concrete (RC) box-girder half-joint bridges are taken as case studies. Both bridges showed signs of deterioration due to age, which led to an in-depth investigation over the last two years by a collaborative effort involving a team from the Italian FABRE Consortium,<sup>30</sup> with members from the Università Politecnica delle Marche (UnivPM) and the University of Camerino (UnicAM), together with a team from ANAS S.p.A., which is the bridge administrator. This collaboration was established within the framework of a research agreement focused on the first applications of the Guidelines 2022 to bridges. The work is organized as follows: at the beginning, after a description of the bridge case studies, a discussion of the whole work is provided, contextualized within the framework of the Guidelines 2022. Then, visual inspections are discussed and the CoA of the bridges is defined. The accurate safety verifications are carried out successfully according to conventional approaches with the addition of in-depth investigations of some structural components, i.e., the prestressing system and the half-joints. In addition, being located in a seismic area, the seismic assessment of bridges is performed as well. This assessment phase configures as a complete and very detailed example of static and seismic verifications of existing prestressed RC box-girder half-joint bridges. Finally, in the last section, the paper presents the monitoring activities and test campaigns conducted to improve the knowledge of the two bridges and to monitor their performance degradation. Several static and dynamic test campaigns were performed over a 2-year period, and a combined dynamic and static SHM system was installed as well. Beyond the information provided by the experimental campaigns, which made it possible to improve the knowledge of the two bridges, the performed activities

provide fundamental support for the planning and managing of the structural safety, as well as for the decision-making process about the bridges' use.

## The Bridge Case Studies

### Description of the bridges

The two bridges are identical side-by-side structures crossing a river and separated by a small longitudinal gap, accommodating a 2-lane carriageway each, forming part of a motorway in Central Italy (Fig. 1). They were designed around the 1970s and built between the end of the 1970s and the beginning of the 1980s. Both the Upstream Bridge (UB) and the Downstream Bridge (DB) are composed of 8 spans for a total length of about 300 m, and they have slightly curved layouts. Spans 1, 2, 6, 7, and 8 are simply supported and about 33 m long, whereas spans 3, 4, and 5 adopt a Gerber scheme with two half-joints located at span 4 (about 60 m long), sustaining a simply supported

30 m long span. The deck of each bridge consists of post-tensioned 3-cell concrete box-girders having constant height for the simply supported decks (2.2 m) and variable height for the Gerber scheme at piers 3 and 4 (varying from 2.7 m in correspondence of the pier to 2.2 m at mid-span).

Five cast-in-place RC diaphragms per span are present, two at the girder ends (80 cm thick) and three distributed along the span length (20 cm thick). Diaphragms are about 9 m spaced and present access holes for inspection purposes. The deck supports are pot-PTFE bearings characterized by different functionalities; fixed, uni-directional, and multi-directional sliding bearings are used to provide a statically determinate scheme. All bearings present a circular rubber layer confined in a pot to allow for rotational movements. The prestressing system is obtained by adopting Morandi cables M5/12, M5/16, and M5/20 (i.e., constituted by 12, 16, and 20 strands, respectively, each one made of 7 wires and characterized by a nominal diameter of 1/2 inch). In detail, 16 cables are used for spans 1, 2, 6, 7, and 8 (8 cables of type M5/12 and 8 of type M5/16), 24 cables for the continuous

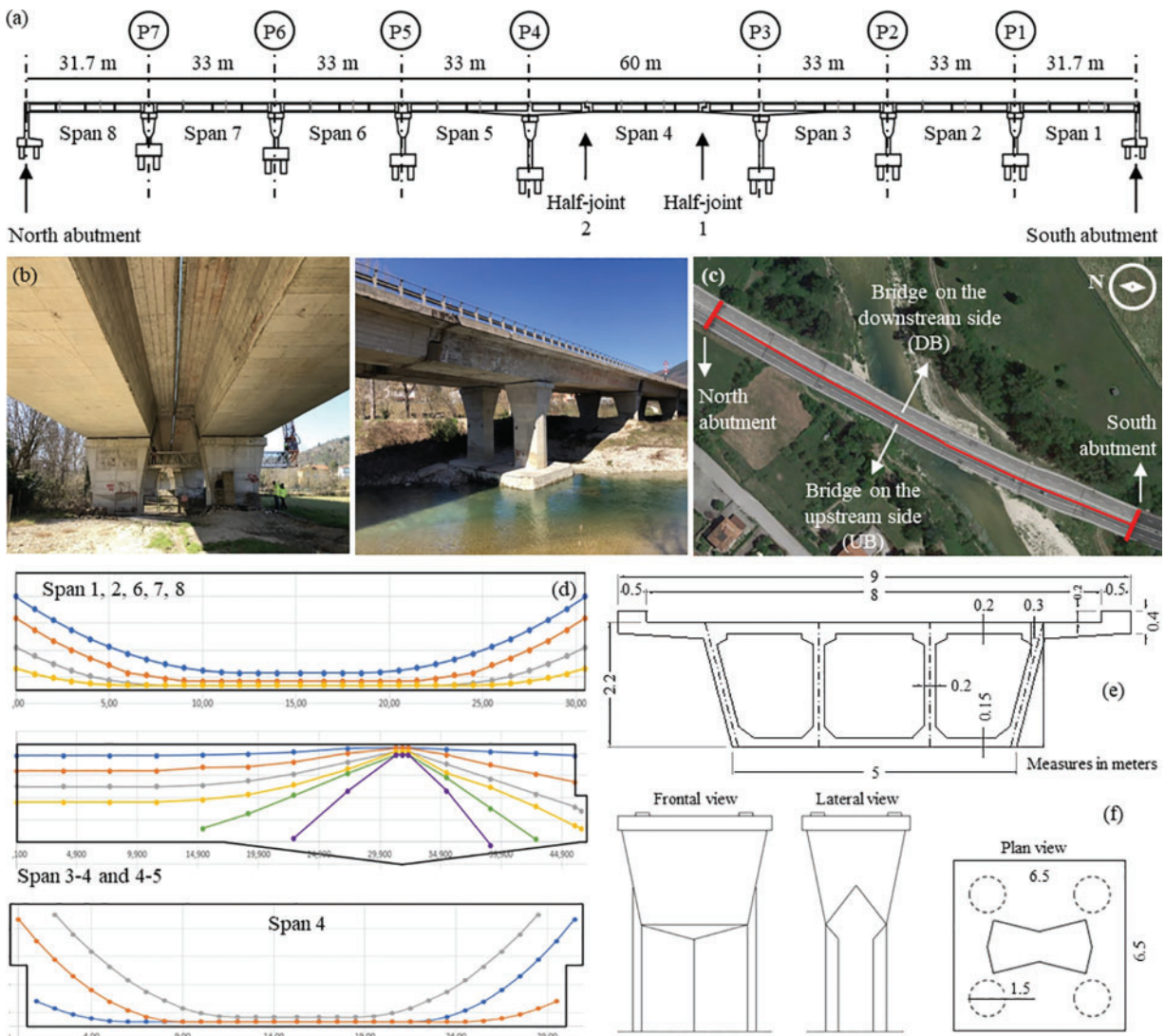


**Figure 1.** Bridges considered as case studies: (a) longitudinal scheme, (b) 2 pictures of the bridges, (c) satellite view (from Google Maps), (d) cable layouts of the prestressing system, (e) mid-span deck cross-section, (f) geometry of piers



Gerber scheme of spans 3, 4 and 5 (of type M5/20), and 12 cables for the span supported by the half-joints within span 4 (4 of type M5/16 and 8 of type M5/20). The RC piers are made with hollow and solid cross-sections of different heights, ranging from about 5 to about 9 m (over the river). Both piers and abutments are founded on 1.5 m diameter RC bored piles.

### **Workflow of the performed activities within the framework of the Italian guidelines**

The bridges are selected as case studies for the comprehensive application of the recently released Guidelines 2022 in the framework of a research agreement between the FABRE Consortium and ANAS S.p.A. The guidelines are based on a multilevel approach that can be divided into three main parts. Part I discusses actions relevant to the preliminary identification of the bridge (census and geo-localization, Level 0), the visual inspection (Level 1), and the definition of the CoA (Level 2). It also contains a preliminary assessment of the structure (Level 3). The primary objective of the CoA is twofold: firstly, to establish a standardized risk classification for bridges across the Italian country, and secondly, to develop a unified rating system for identifying urgent safety measures and prioritizing maintenance interventions.

Part I of the process entails on-site visual inspections of bridges, supplemented by special inspections when necessary, such as for post-tensioned RC bridges. In detail, special inspections for post-tensioned bridges foresee a multilevel experimental campaign aimed at investigating the defective state of the prestressing system; non-destructive and semi-destructive tests can be used to identify the cables layout, the presence of voids in injections, the oxidation and corrosion on ducts and cables, the concrete corrosion potential and, eventually, the cable residual areas. Evaluation at Levels 0, 1, and 2 was conducted for the bridge case studies by a joint team comprising personnel from FABRE and ANAS, resulting in the definition of the CoA. Special inspections have not been carried out yet, but they are planned for the near future; however, the CoA of the bridges resulted in the highest possible (High), and consequently, it is not conditioned by the special inspection results, which are in any case mandatory for the prestressing system. Considering the obtained CoA, the Level 3 assessment has not been performed in favor of the accurate assessment (Level 4), which is mandatory for bridges falling into the High CoA.

Part II outlines recommendations for assessing the load-bearing capacity of bridges (Levels 4 and 5) in accordance with the Italian technical code and the Guidelines 2022. The latter introduces different performance levels for existing bridges (ranging from adequate, operative, and transitable bridges), along with the concept of a “reference time” that is used to calibrate the partial safety factors adopted for safety verification purposes. Depending on the performance level (i.e., for the adequate, operative, and transitable conditions), suitable partial safety factors and loads are defined to perform the safety assessments, reducing values from adequate to transitable conditions. Operational and transitable conditions are defined within specific time frames (30 and

5 years, respectively), necessitating periodic re-evaluation or the implementation of safety measures, such as repairs or load restrictions.

Part III offers recommendations for testing and monitoring activities throughout the lifespan of a bridge. Short-term and long-term monitoring suggestions are provided, along with recommendations for static and dynamic performance assessments. The bridges under investigation have undergone extensive surveillance activities, including both static and dynamic testing. Additionally, a permanent monitoring system has been installed as well. A summary of the experimental activities and their alignment with the Guidelines 2022 is presented in Fig. 2. As can be seen, many activities have been performed from March 2022 dealing with Part III of the Guidelines 2022. For this reason, the strength of this document is to pay more attention to the discussion of these activities, while providing less detail for those of Parts I and II. The latter, however, have been extensively treated for the safety assessment of the two bridges. Readers interested in further examining the general aspects of Parts I and II may refer to the numerous articles reported in the literature review in the introduction.

### **Inspection Activities and Class of Attention**

In February 2022, visual inspections were conducted on the two bridges following the Guidelines 2022 prescriptions and procedures. The inspections involved visually assessing of all the structural elements of the bridges, together with non-structural components, such as pavement joints and accessories (e.g., guardrails, drainage system, equipment, etc.). Each structural element has a standardized inspection form to be filled out to record information about deterioration phenomena and damage observed during the visual inspections. The inspection forms vary based on the type and material of the structural component; from a general point of view, they include a list of typical defects that were selected based on the technical literature, administrator’s manuals, and real experiences on existing bridges.

A weight is assigned to the gravity of each defect (denoted as  $G$ ), which ranges from 1 to 5 on an increasing severity scale. In addition, parameters for the defect extent ( $k_1$ ) and intensity ( $k_2$ ) are introduced, which can take values equal to 0.2, 0.5, or 1, based on an increasing severity scale. For critical defects (i.e., for  $G$  equal to 4 or 5), it is also possible to indicate whether the overall stability of the structure is compromised by selecting a specific checkbox (PS). For each defect, the inspection form includes fields for the photo ID, any observations, and whether the defect is absent because it is not applicable (NA), not detectable (NR), or simply because it is not present (NP). An example of an inspection form with some of the most significant defects for prestressed RC beams is provided in Table 1.

The two bridges are characterized by critical elements in accordance with the Guidelines 2022: the post-tensioning system and the half-joint spans. From the visual inspections, it was observed that the simply supported spans were in a fair state of conservation with defects mainly related to

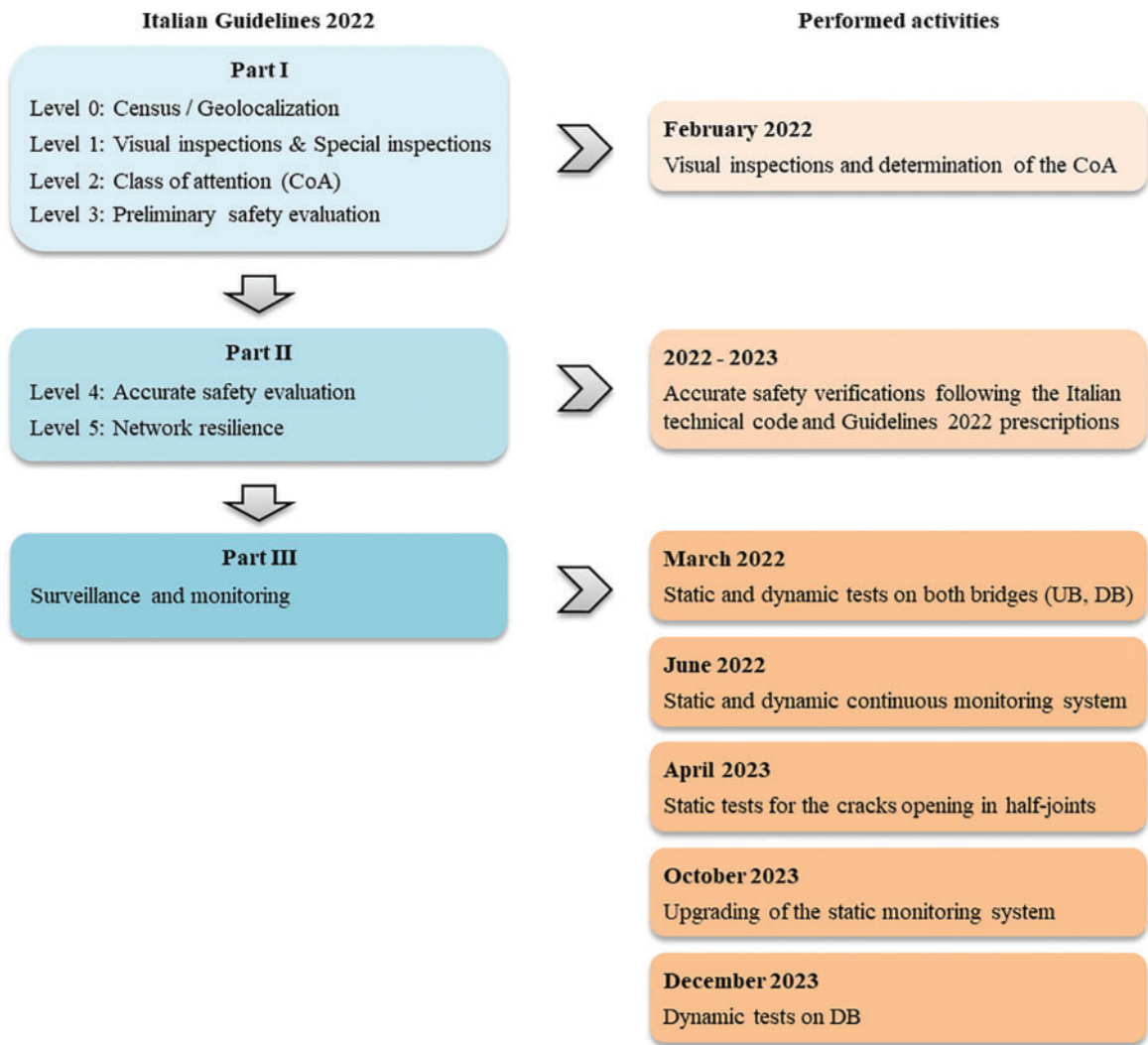


**Figure 2.** Italian Guidelines 2022 framework and the relevant activities performed on the bridge case studies

**Table 1.** Extract of the inspection form for RC and prestressed beams.

		Prestressed RC beam													
Applicability	Defect description	Check	Weight	G	Intensity			Extension		Photo	ID	PS	NA	NR	NP
					k2	k1	k1	k1	k1						
RC/prestressed	Active humidity traces	<input type="checkbox"/>	3	<input type="checkbox"/>	<input type="checkbox"/>	<input type="checkbox"/>	<input type="checkbox"/>	<input type="checkbox"/>	<input type="checkbox"/>	<input type="checkbox"/>	<input type="checkbox"/>	<input type="checkbox"/>	<input type="checkbox"/>	<input type="checkbox"/>	<input type="checkbox"/>
RC/prestressed	Concrete degradation	<input type="checkbox"/>	3	<input type="checkbox"/>	<input type="checkbox"/>	<input type="checkbox"/>	<input type="checkbox"/>	<input type="checkbox"/>	<input type="checkbox"/>	<input type="checkbox"/>	<input type="checkbox"/>	<input type="checkbox"/>	<input type="checkbox"/>	<input type="checkbox"/>	<input type="checkbox"/>
RC/prestressed	Reinforcement oxidation/corrosion	<input type="checkbox"/>	5	<input type="checkbox"/>	<input type="checkbox"/>	<input type="checkbox"/>	<input type="checkbox"/>	<input type="checkbox"/>	<input type="checkbox"/>	<input type="checkbox"/>	<input type="checkbox"/>	<input type="checkbox"/>	<input type="checkbox"/>	<input type="checkbox"/>	<input type="checkbox"/>
Prestressed	Duct exposure	<input type="checkbox"/>	2	<input type="checkbox"/>	<input type="checkbox"/>	<input type="checkbox"/>	<input type="checkbox"/>	<input type="checkbox"/>	<input type="checkbox"/>	<input type="checkbox"/>	<input type="checkbox"/>	<input type="checkbox"/>	<input type="checkbox"/>	<input type="checkbox"/>	<input type="checkbox"/>
Prestressed	Duct degradation and tendon oxidation	<input type="checkbox"/>	4	<input type="checkbox"/>	<input type="checkbox"/>	<input type="checkbox"/>	<input type="checkbox"/>	<input type="checkbox"/>	<input type="checkbox"/>	<input type="checkbox"/>	<input type="checkbox"/>	<input type="checkbox"/>	<input type="checkbox"/>	<input type="checkbox"/>	<input type="checkbox"/>
RC/prestressed	Diagonal crack	<input type="checkbox"/>	5	<input type="checkbox"/>	<input type="checkbox"/>	<input type="checkbox"/>	<input type="checkbox"/>	<input type="checkbox"/>	<input type="checkbox"/>	<input type="checkbox"/>	<input type="checkbox"/>	<input type="checkbox"/>	<input type="checkbox"/>	<input type="checkbox"/>	<input type="checkbox"/>
RC/prestressed	Vertical crack	<input type="checkbox"/>	5	<input type="checkbox"/>	<input type="checkbox"/>	<input type="checkbox"/>	<input type="checkbox"/>	<input type="checkbox"/>	<input type="checkbox"/>	<input type="checkbox"/>	<input type="checkbox"/>	<input type="checkbox"/>	<input type="checkbox"/>	<input type="checkbox"/>	<input type="checkbox"/>
Prestressed	Prestressing system tendon reduction	<input type="checkbox"/>	5	<input type="checkbox"/>	<input type="checkbox"/>	<input type="checkbox"/>	<input type="checkbox"/>	<input type="checkbox"/>	<input type="checkbox"/>	<input type="checkbox"/>	<input type="checkbox"/>	<input type="checkbox"/>	<input type="checkbox"/>	<input type="checkbox"/>	<input type="checkbox"/>

water infiltration through non-sealed pavement joints and damaged drainage systems. These defects included traces of both active and passive humidity, concrete degradation,

oxidation, and corrosion of reinforcements. Additionally, concrete spalling in areas subjected to humidity and drying cycles was detected as well, e.g., in the cantilevered

portion of the concrete slabs. In correspondence with the Gerber spans (spans 3, 4, and 5), an evident permanent deflection was observed (Fig. 3a) with a greater lowering at span 4 of both bridges, presumably related to concrete creep and/or excessive loss of prestress in combination with poor concrete quality. This lowering exposes the structures to significant dynamic effects deriving from the passage of heavy vehicles, potentially increasing fatigue effects on the structures. Moreover, the half-joints and the post-tensioning system exhibited defects such as (i) the complete gap closure at the half-joints (Fig. 3b), resulting in the development of an inner and undesirable stress state on the deck, (ii) the presence of moisture traces and white efflorescence along the longitudinal path of the prestressing cables (Fig. 3d), which could be attributed to water infiltration within the ducts or at the interface between ducts and concrete, (iii) and the presence of cracks close to the half-joints (Fig. 3c) at the inner corner of the nib and the lower corner of the nib full-depth interface, similar to those associated with half-joint collapse mechanisms reported in the literature.<sup>31,32</sup> Also, the DB showed an important deformability of the cantilever beams of span 4 under heavy vehicular traffic and, in the cracked half-joint, the opening and closing phenomena of cracks on the lateral side of the box-girder were noted during the passage of heavy vehicles, also producing noise and concrete dust fall.

Data collected during visual inspections, together with those collected by the road administrator and inherent to the road and infrastructure characteristics (e.g., level of traffic, importance of the road, age, codes adopted for the bridge design, maintenance activities, surrounding territory characteristics, etc.), are used to achieve the global CoA. The

latter is a combination of several partial CoAs obtained for 4 types of risks to which the structure may be subjected: the structural and foundational risk, the seismic risk, the hydrological risk, and the landslide risk. A summary of the partial CoAs and the global one obtained for the two bridges at hand is reported in Table 2. It is worth noting that for the definition of landslide and hydrological risks, on-site inspections were carried out by engineers with expertise in both fields. The area surrounding the viaduct is classified, in terms of physiographic units, among the ‘hill areas’, i.e. areas at low altitudes, frequently with a low morphology due to the presence of relatively erodible formations. The slope is moderately steep ( $10^{\circ}$ – $25^{\circ}$ ), and the area is characterized by a relatively extensive, terraced alluvial valley. These considerations led to the adoption of a Low CoA for the landslide risk. The hydrological CoA is assigned as a function of the overtopping phenomena or insufficient hydraulic franking and of erosive effects, whether generalized or localized. Being flanked, the two bridges are considered as a unique system and the obtained hydraulic CoA is Medium-High.

Based on visual inspection outcomes (and also on safety verification outcomes, as will be shown in the sequel), the road administrator decided to close the DB and move the relevant traffic to the UB to guarantee at least one traffic lane in each direction of the route. As a result of this decision, monitoring actions were considered for the UB to improve the understanding of the bridges’ behavior and to support decisions regarding the use of the open bridge in the transitory period.

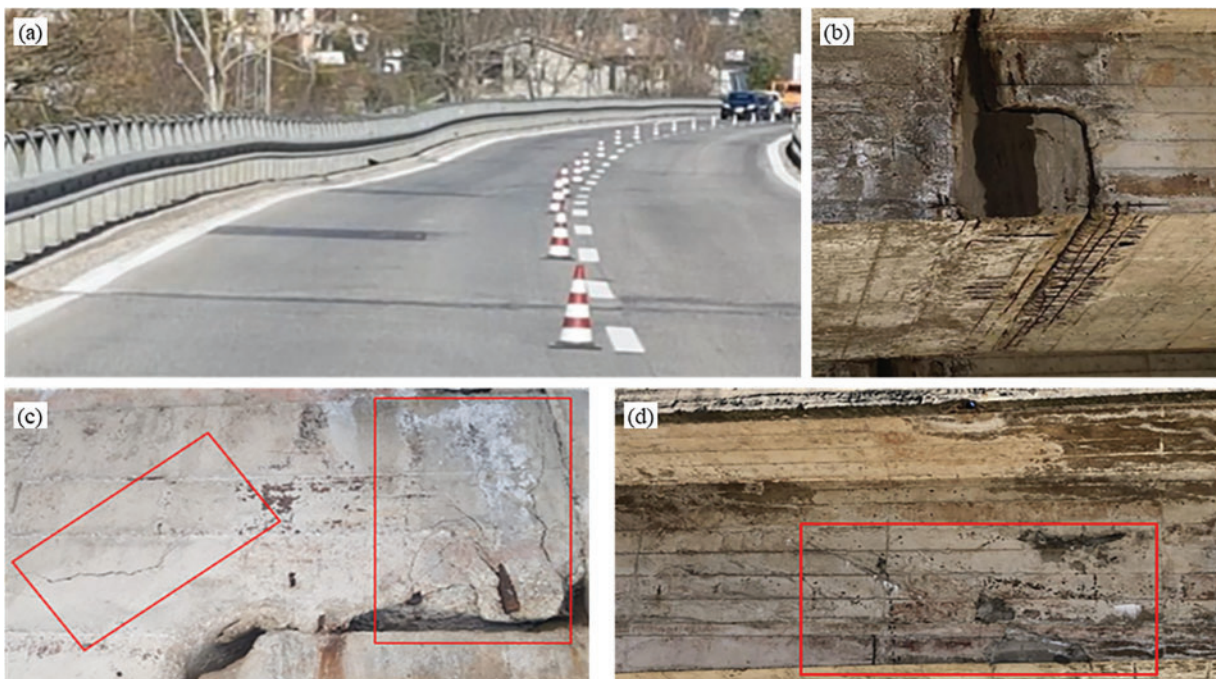


**Figure 3.** Defects detected during the visual inspections: (a) permanent lowering of span 4, (b) defects of the half-joints, (c) cracks in correspondence of the half-joints, (d) efflorescence along the longitudinal path of the prestressing cables



**Table 2.** Determination of the partial and global CoA of the two bridge case studies

Bridge	Partial CoA				Global CoA
	Structural and foundational	Seismic	Landslide	Hydraulic	
DB	High	High	Low	Medium-High	High
UB	High	High	Low	Medium-High	High

## Evaluation of the Bridge Safety

### Preliminary phases and structural modeling

The Guidelines 2022 foresee that for bridges falling within a High CoA, in-depth safety verifications must be carried out in accordance with Level 4. The safety assessment of the two bridges is performed evaluating the structural performance under both static and seismic actions, following the Guidelines 2022 and the NTC18<sup>33</sup> regulations. It is worth noting that the Italian NTC18 regulations are derived from Eurocodes, and, therefore, the requirements of the two codes are very similar. The static assessment of the bridge deck is performed considering the adequate performance level for the bridge, i.e., considering a bridge that satisfies the actual code verifications at the Ultimate Limit State (ULS) and that can be used without any traffic restrictions. As for the decks, three main components are verified: (i) the simply supported span (representative of spans 1, 2, 6, 7, and 8), (ii) the continuous Gerber girder with half-joints (spans 3, 4, and 5), and (iii) local verifications of the half-joints and the transverse bending of the box cross-section. Furthermore, an in-depth investigation of the prestressing effects is conducted, trying to understand the reasons for the lowering of spans 4 for both bridges, as well as the seismic verification of the whole structure is performed. Foundations and abutments are not verified following the Italian technical code, for which, in existing bridges, the assessment

of foundations may be omitted if no significant and critical situations directly related to the soil-foundation systems are found.

To enhance knowledge of bridges, a detailed investigation of material mechanical properties was performed together with a collection of information from existing design documents. This included extracting concrete cores and steel samples from various bridge components and conducting tests to assess the condition, integrity, and residual tension of cables. The highest knowledge level (LC3) in accordance with the Italian technical code is reached; therefore, a unit confidence factor is applied to determine the design material mechanical properties, namely, no reduction is done.

The analysis considers typical bridge loads, including dead loads, permanent loads, traffic loads (similar schemes foresaw in the Eurocodes), wind loads, temperature variations, and seismic actions. The structural analysis is performed by adopting the SAP2000 software, and developing different models depending on the verifications to be carried out (Fig. 4). In particular, considering the bridge static scheme, which consists of a series of independent decks, two separate models are prepared for the static global analysis, one representative of all the simply supported spans (Fig. 4a), and the other of the Gerber spans (Fig. 4b). The Finite Element Models (FEMs) are developed by using frame elements, which have the great advantage of directly providing stress resultants along the elements. In the modeling, the geometry of the structure is reproduced as closely

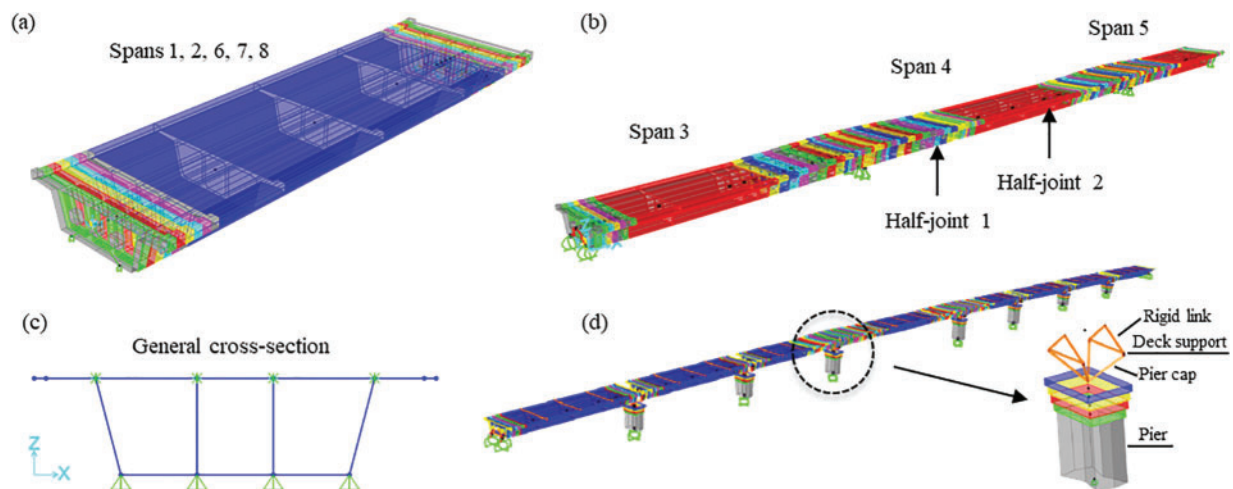


**Figure 4.** Developed FEMs for the bridge case studies (extruded view): (a) model for simply supported spans, (b) model for Gerber girders, (c) plane model for the analysis of the transverse local effects, (d) global model for the seismic analysis

as possible, taking into account the geometric variation of the cross-sections. To this end, the deck is discretized with a series of frame elements positioned, for the sake of simplicity, at the centroid of the mid-span cross-section. The elements are able to account for the flexural and shear deformability, as well as for the primary torsion effects. On the contrary, torsional warping effects and the deck distortion are neglected. The deck is modelled as simply supported, and roller and pinned restraints are used on the basis of the real support layout. The analysis of the overall models is completed by the transverse analysis of the deck to identify the effects induced by the transverse bending. The prestressing forces are taken into account, exploiting the software potentials: stresses in the prestressed system are used for evaluating the relevant contribution to the beam shear capacity, while they are neglected for computing the ultimate flexural capacity by only checking for the ultimate strain of strands.

The evaluation of local effects due to the transverse bending of the deck cross-section is carried out with a plane frame model, assuming a fixed node scheme (Fig. 4c) supported at the level of the cross-section webs and subjected to vertical loads due to permanent and traffic actions distributed to maximize positive and negative bending moments on the top slab and the webs; the thermal actions are also considered. For the seismic analysis, a global model of the entire viaduct is developed to capture the overall behavior of the structure and the interaction between the different structural components (Fig. 4d). In the spatial model, all structural elements are modeled using frame elements. Piers are fixed at the base, and the pier caps are modeled with rigid link elements, considering the real position of the bridge support devices through which actions at the deck level are transferred to substructures. The bridge has a curvature in plan which, although not accentuated, is taken into account in the global modelling. For all models, the material mechanical properties are set equal to the mean values obtained from tests on samples collected on-site.

### **Static assessment of the bridge deck**

The static assessment is performed by comparing the maximum bending moments and shear forces acting along the deck with the corresponding resistant bending moment and resistant shear force. Moreover, in view of the cross-section typology, the shear demand on the box-girder webs is evaluated considering the superposition of shear force and torsion arising from the non-symmetric distribution of the traffic loads over the deck, maximizing both actions. Exploiting the influence lines, both positive and negative values of each stress resultant (i.e., shear force and torsion) are maximized considering the relevant concomitant values. Furthermore, the local effects due to the transverse bending are considered for the web checks. In detail, this verification is performed taking into account the edge web of the box cross-section that, for a non-symmetrical traffic load configuration, is the one mostly excited, subjected to shear stresses due to both

shear forces and torsion, as well as to transverse bending due to the load distribution over the deck. It is worth mentioning that the shear stresses due to torsion are evaluated considering the multicellular cross-section equilibrium and congruence. The verification is then carried out by comparing the transverse bending moment demand with the capacity; the latter is calculated considering the stirrup legs on the tensile side of the web. The amount of residual reinforcement corresponding to the stirrups on the compressed side and any excess in the transverse bending verification are considered in the shear and torsion verification. The contribution of the inclined prestressed cables is also suitably taken into account in the safety assessment. The flexural and shear capacity of members are evaluated according to standard methods for RC elements suggested by both the Italian NTC18 and the Eurocodes.

A summary of the verification outcomes is illustrated in Fig. 5, where red areas are used to identify those sections of the deck where at least one of the aforementioned verifications is not satisfied. If some verifications are not fulfilled considering the adequate bridge conditions, they should be repeated considering less severe situations, such as operational or even transitable bridge conditions. The former approach uses codified movable loads with adjusted safety factors, while the latter restricts bridge use and allows for less demanding movable loads with adjusted safety factors. Retrofitting is required for operational and transitable bridges within 30 and 5 years, respectively. Being the bridges at hand verified as transitable, the road administrator chose to demolish and rebuild them. Meanwhile, a continuous monitoring system was installed on one bridge (UB) to ensure safe usage, following the Guidelines 2022. The latter will be discussed in the sequel.

### ***In-depth investigation of the prestressing system of Gerber girders***

Due to pronounced deflection in span 4 (Gerber scheme), the impact of prestressing on deck deformation is analyzed, trying to correlate the evident lowering to the intrinsic characteristics of the structure and/or to the prestressing system. Starting from the model of spans 3, 4, and 5 (Fig. 4c), prestressing cables are added by using the “Tendon” element command and by considering their actual layout, both planimetrically and altimetrically (Fig. 6a). Prestressing forces acting on cables are estimated starting from the results of the experimental campaign performed to acquire data on the mechanical properties of construction materials. Specifically, de-tensioning tests were performed on 4 wires of different cables, obtaining residual tension values around 630–810 MPa.

Two typical situations are analyzed: (i) the bridge subjected to dead and permanent loads together with the prestressing forces and (ii) the addition of long-term effects due to creep effects. The applied prestressing forces in phase (i) are reduced by friction losses. Deformed profiles of Fig. 6b are plotted only for the Gerber beams, while



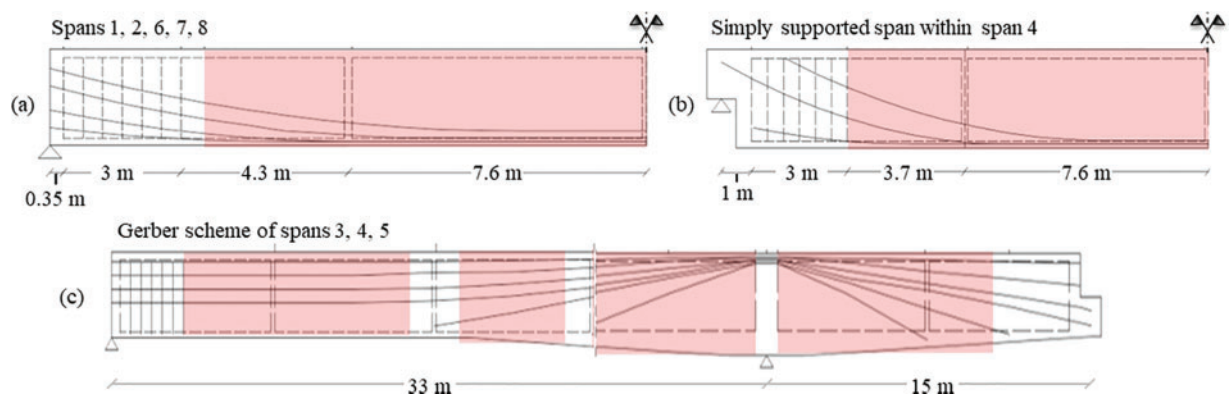


**Figure 5.** Results of the static assessment on the deck: (a) typical simply supported span, (b) simply supported span within span 4, (c) Gerber girders

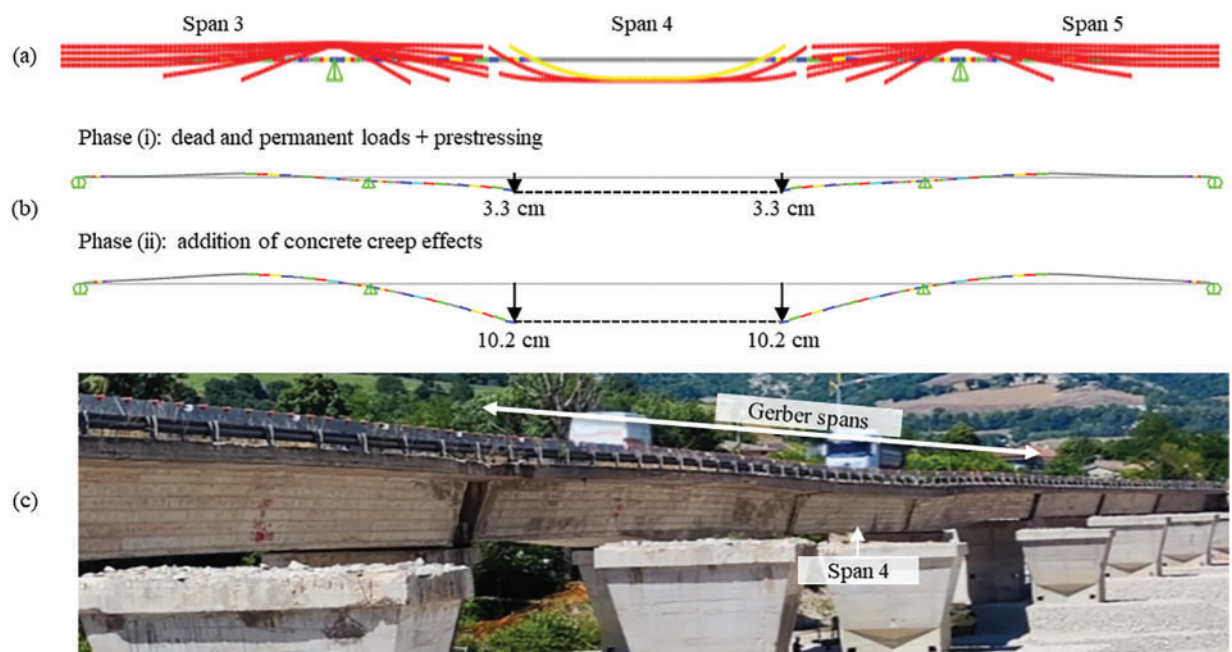


**Figure 6.** Numerical investigation of the downward deflection of the Gerber scheme spans: (a) developed FEM, (b) analyses in two different phases, (c) on-site picture of UB after the DB demolition

the suspended deck is drawn undeformed. Indeed, on-site pictures (Fig. 6c) reveal that the simply supported beam of span 4 does not show any evident deflection. In phase (i), the tendons layout and prestressing fail to ensure upward deflection under permanent structural and non-structural loads, causing the deck to lower by a maximum of 3.1 cm at the half-joints. In phase (ii), creep effects are added following the Eurocode 2,<sup>34</sup> which amplifies the initial elastic deformation by a coefficient of 3.3, resulting in a maximum lowering of 10.2 cm. This estimation is conservative as it does not account for the reduction in prestressing due to creep. The numerical displacement profiles (Fig. 6b) match the observed ones during visual inspections (Fig. 6c), indicating that the downward deflection of the deck in the Gerber scheme is primarily caused by the design layout of the prestressing tendons and the cumulative effects of long-term concrete creep instead of damage to the structure.

### Local verifications of the half-joints

The verification of the half-joints is based on strut and tie models identified on the basis of the rebar layout found in the construction drawings. Two different types of rebar layouts can be recognized for the end diaphragms hosting the half-joints, one adopted for the sections in correspondence of the box-girder webs (henceforth referred to as ribs) and one for the cell sections between the webs (henceforth referred to as cells). A summary of the main geometric and rebar characteristics is illustrated in Fig. 7a. It is worth explaining that the simply supported deck of span 4 is supported on two devices at each half-joint. Considering the reinforcement layout and suggestions of Eurocode 2, two types of 3D strut and tie models are considered (Fig. 7b): the first (model 1) is suitable for both rib and cell layouts, while the second (model 2) is only for ribs. Exploiting the box-girder transverse symmetry, the strut and tie spatial models are shown in Fig. 7c

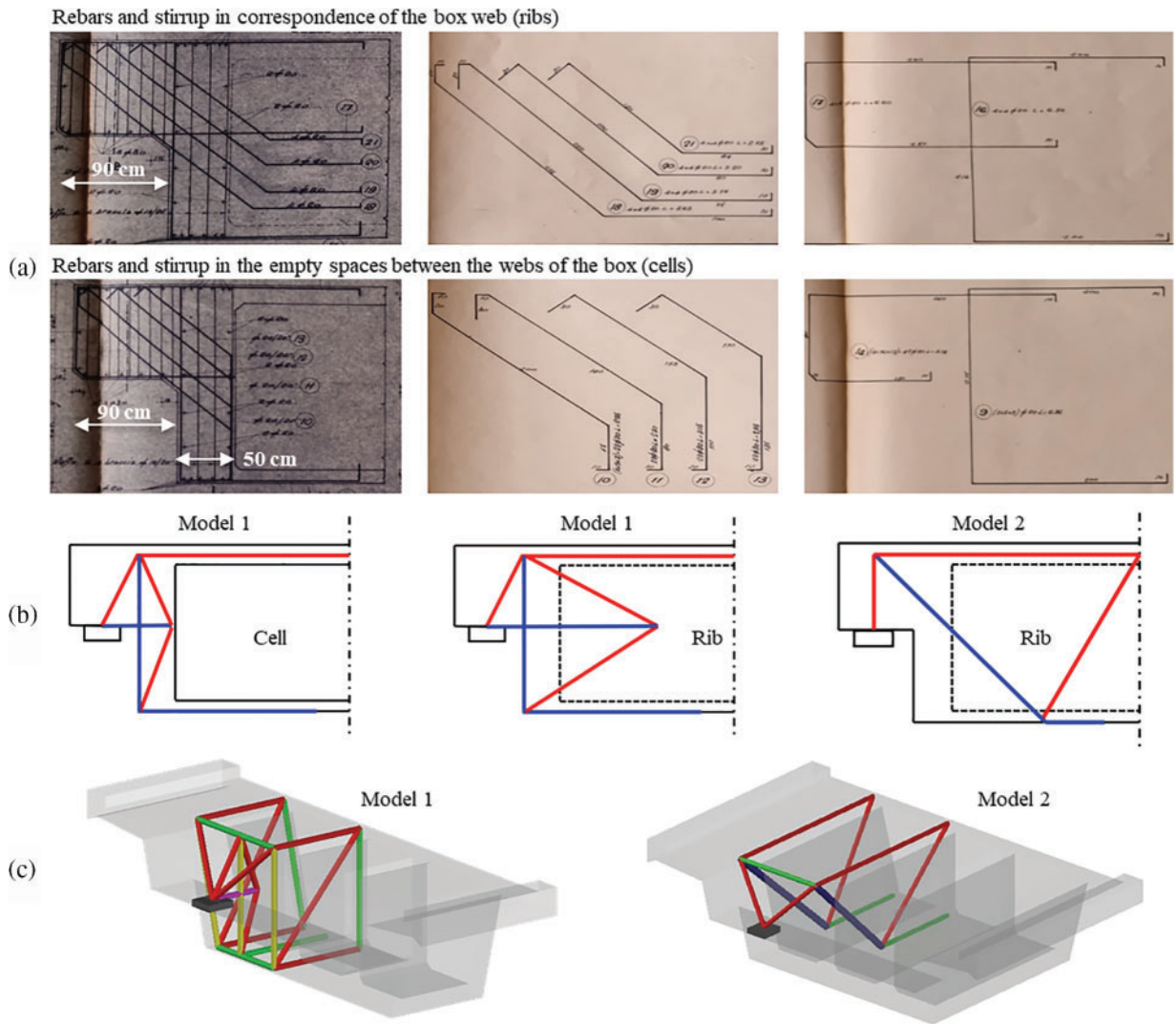


**Figure 7.** Verification of half-joints: (a) half-joint geometry and rebar layouts, (b) strut and tie models from Eurocode 2, (c) spatial strut and tie models for the bridges at hand

only for one of the two supports at each half-joint cross-section. From the schematization of model 1, it is possible to observe that, at the support node, all the trusses converge at a point where equilibrium is guaranteed by the presence of the horizontal reinforcements that are the elements governing the crisis of model 1. The global resistance of the half-joint is the sum of the resistance arising from model 1 and model 2, and, for convenience, it is expressed in terms of vertical force acting in correspondence with the support. The latter is compared with the restraint reaction at the support due to dead, permanent, and traffic loads acting on the deck. For the two bridges, the check is always satisfied, with the lower safety factor equal to 1.4.

### Seismic assessment of the overall bridges

The seismic assessment of both bridges is conducted by considering the shear forces and bending moments on piers due to the seismic excitation in conjunction with the vertical actions at seismic conditions. A dynamic analysis with a seismic response spectrum is adopted to determine the seismic

demand. The NTC18 prescribes to combine the contribution of vibration modes that mobilize at least 5% of the seismic mass for a total mobilized mass not lower than 85% of the total mass. Hence, 27 vibration modes are taken into account. Then, the seismic action is combined into the three main orthogonal directions of the structure by summing 100% of the action in the main direction with 30% in each of the other two directions.

Two different types of verifications are performed separately, considering the biaxial bending and the shear forces acting at the pier basis. For the former verification, the behavior factor used to obtain the design spectrum is assumed to be equal to 2.0, while 1.5 is assumed for the latter verification. The axial force acting on piers is that produced by the application of permanent loads only. The biaxial bending resistance domain is determined by considering the actual number and layout of longitudinal rebars of the pier base cross-sections. These are different for the two pier typologies, i.e., with hollow and solid cross-section, and they are reported in Fig. 8a. The verifications are not satisfied

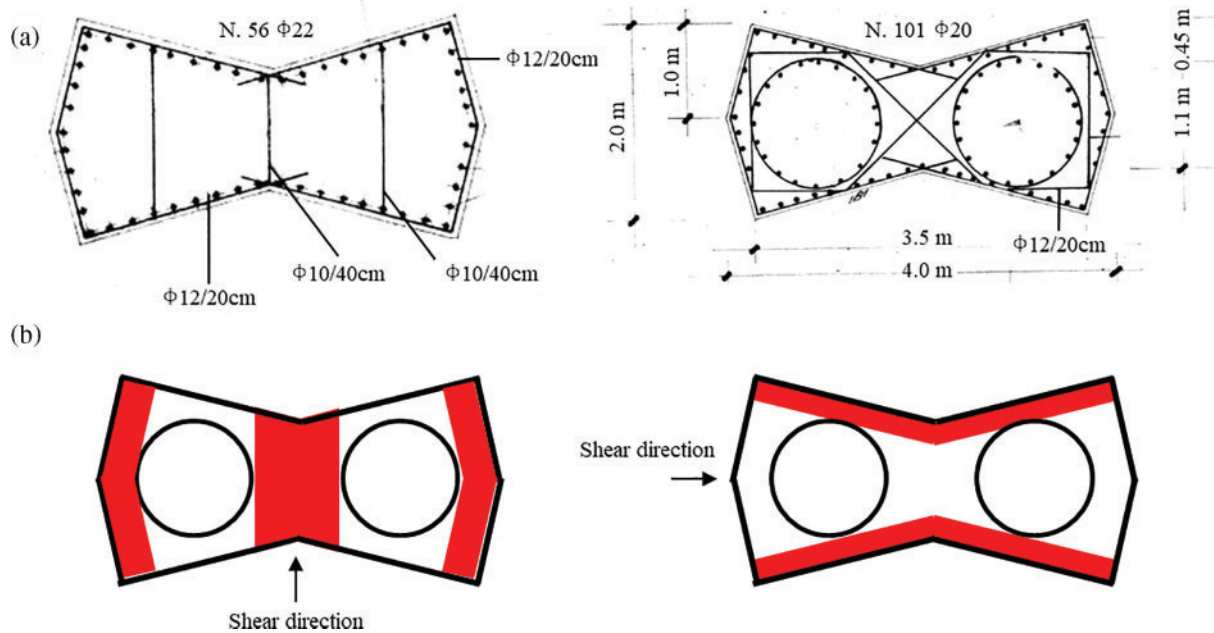


**Figure 8.** Seismic verification on piers: (a) geometric dimensions and rebar layouts for the typical solid and hollow pier, (b) shear transverse zone considered for the shear verification on hollow piers

for piers P1, P2, P3, P4, and P5 when the seismic action is acting mainly in the transverse direction of the bridge, are not satisfied for P3 for the seismic action acting mainly in the longitudinal direction, while are always satisfied for the seismic action acting mainly in the vertical direction. The shear verification at the pier bases is performed by calculating the shear resistance with the formulae provided by the NTC18 and considering the number of stirrup legs located within the shear transfer zones, extending from the compressive to the tensile chords. The latter comprise the overall cross-section for the solid piers and only some sub-parts for the hollow ones, as highlighted in Fig. 8b for the two main orthogonal directions. The shear resistance in the two main orthogonal directions of the bridge piers (transverse and longitudinal) is generally greater than the relevant seismic demand, except for P3 in the transverse direction, where the verification is not satisfied. In any case, the shear verifications provide better results than the biaxial bending ones.

## Experimental Campaigns and Continuous Monitoring

The two bridges have been the object of several test campaigns during the 2022–2023 years to improve the knowledge and, consequently, to reduce uncertainties in the safety evaluations, consistently with indications provided by the Guidelines 2022. These tests aimed to deepen the understanding of the bridges' behavior and to gather data crucial for making informed decisions regarding their use in the transitory period, especially with reference to the open bridge (UB). A summary of the whole experimental campaign is reported in the right-hand side of Fig. 2. The

different experimental campaigns are described below, and the main results obtained are discussed.

### Static and dynamic tests on both bridges

In March 2022, an experimental campaign began after visual inspections showed significant deformability of the DB under heavy traffic. Extensive static and dynamic tests were conducted on both bridges. The DB was closed to traffic for a whole day and static tests were preliminary performed. A 33.5 t heavy truck was stationed for about 10 minutes at three different points of the longest span (in correspondence with the two half-joints and at mid-span), and the vertical displacements of the loaded points were measured (Fig. 9). Experimental data are compared with numerical results from two FEMs: one initially developed for static deck assessment (Fig. 4b), and another modified version where gaps at half-joints are closed to entrust bending moments. This modification alters the Gerber scheme to a continuous beam scheme, restricting half-joint rotations practically. Comparison (illustrated in Fig. 9) shows that the amount of experimental vertical displacements due to the load moving along the deck is much similar to the numerical ones obtained by considering a continuous scheme. In contrast, the displacement profile is consistent with none of the two models, suggesting that the real condition for the two half-joints is midway between the two models, assuming perfect boundary conditions. Thus, it may be reasonably asserted that the obtained experimental data are affected by the half-joint conditions, characterized by closed gaps, with beams practically in contact with each other. As a consequence, the boundary conditions of the suspended girder are capable of restraining the beam rotation with a consequent transferring of bending moment. Hence, the non-perfect



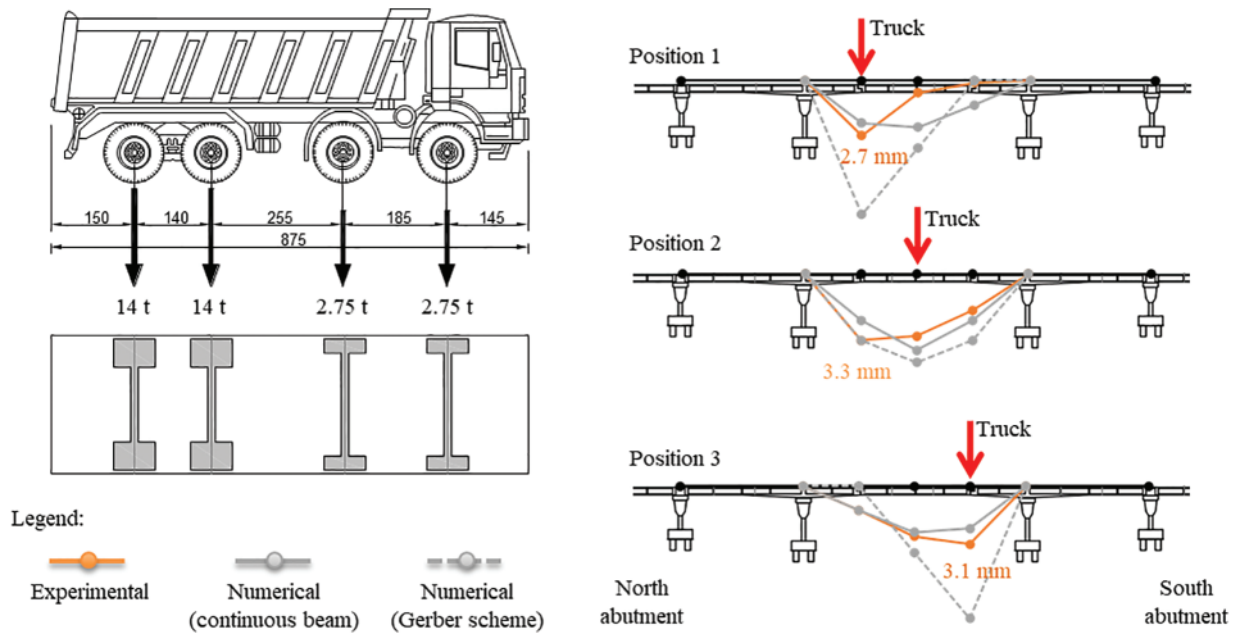


**Figure 9.** Results of the static load tests performed on the main span (Span 4) of DB (dimensions of truck geometry are in cm)

non-symmetric boundary conditions offered by the two half-joints at the edges of the simply supported beam are probably the most responsible for the non-symmetric response of the span during the proof load.

On the same day, dynamic tests were conducted as well. At first, Ambient Vibration Tests (AVTs) were performed on both bridges. These tests consist of deploying a sensor array over the bridge deck (generally accelerometers) and measuring the vibrations due to the so-called ambient noise, i.e., vibrations produced by anthropic (e.g., traffic, works) and natural (e.g., wind, ground microtremors) activities. Then, thanks to Operational Modal Analysis (OMA) techniques<sup>35</sup> (specifically the covariance-driven stochastic subspace identification-SSI-COV-method),<sup>36</sup> the modal parameters that characterize the dynamic behavior of the structure are identified, namely the resonance frequencies with the relevant mode shapes and damping ratios of each vibration mode. The adopted sensor configurations are shown in Fig. 10a: 25 cross-sections were instrumented for both structures even if different sensor layouts were used. Indeed, for DB, three accelerometers per section were employed, two measuring in the vertical direction and positioned on the lateral kerbs of the deck to capture modal displacement components due to bending and torsional modes, one measuring in the transverse direction to detect modal displacement components due to transverse vibration modes. For UB, a reduced number of sensors was adopted due to traffic. However, the adopted number of sensors was sufficient to verify that the UB dynamics were very similar to the DB one. It is worth noting that during the AVTs, the DB was closed to traffic, which was completely redirected on UB, and consequently, the two bridges were subjected to different levels of anthropic excitations, obviously greater (in terms of acceleration amplitudes) for the UB. This may be

responsible for the slightly different fundamental resonance frequencies identified for the two bridges. Indeed, focusing on the first mode (Fig. 10b), which is a pure bending mode involving the Gerber girders (span 3, 4, and 5), a lower value of the identified frequency is obtained for the UB; this is consistent with the fact that higher vibrations due to traffic can trigger a slight reduction of the structure initial tangent stiffness and enhance the damping capability, due to the activation of small dissipative mechanisms.<sup>37</sup> This effect is also evident in the modal damping ratio, which is a little higher for the UB. Instead, mode shapes, as expected, are almost identical. Summarizing, no substantial variations in the dynamic behavior of the bridges were observed.

After AVTs, dynamic tests recorded deck vibrations from truck passages on the closed DB. Accelerometers at section 14 were kept in place to record vibrations from multiple truck passages at a constant speed of 80 km/h. Accelerations recorded by the two sensors measuring in the vertical direction are plotted on the top of Fig. 11a. It is worth observing that they resemble signals obtained from impact tests with the relevant free-damped oscillations; this behavior is heightened by a discontinuity over the deck pavement in the proximity of the half-joint. The Short Time Fourier Transforms (STFTs) of the acceleration time histories are also plotted in Fig. 11a. The signals reveal significant frequency content around 1.78 Hz, corresponding to the deck's fundamental resonance frequency, associated with a pure bending mode involving the Gerber girders, similar to that identified by OMA. The latter shows a significant frequency content (highlighted with a dashed red line) around 1.78 Hz, corresponding to the fundamental resonance frequency of the deck (pure bending mode involving the Gerber girders, almost the same as identified by OMA). The signals from vertical accelerometers, filtered around the fundamental

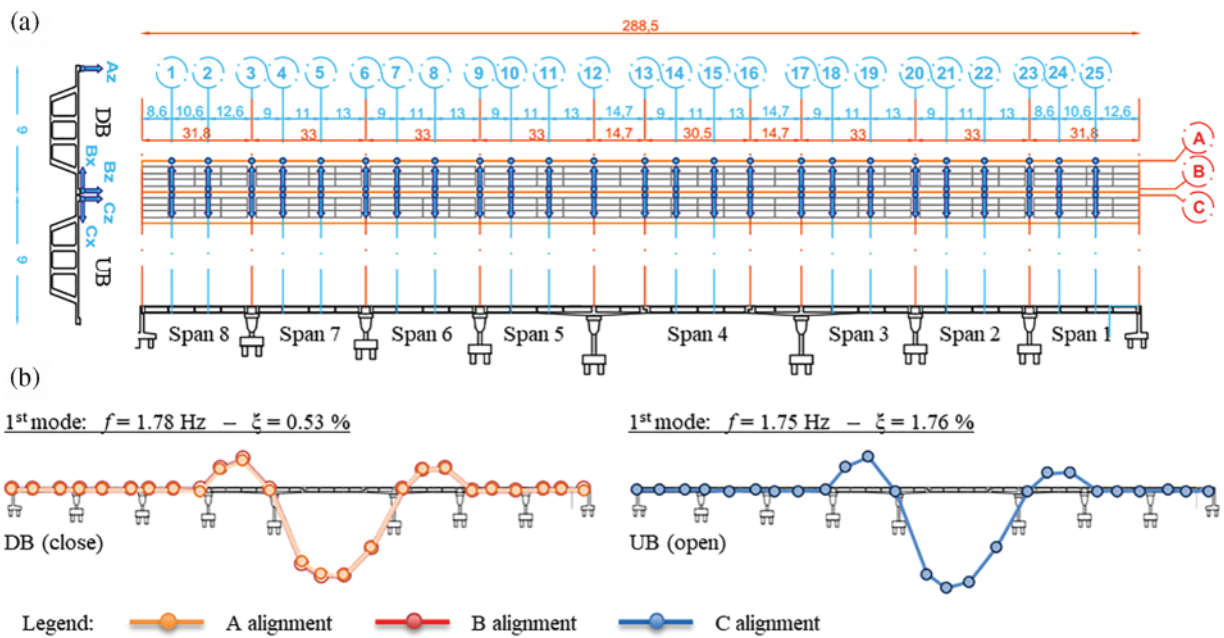


**Figure 10.** AVTs for both bridges: (a) sensor configurations (measurements are in m), (b) identified modal parameters for the fundamental vibration mode

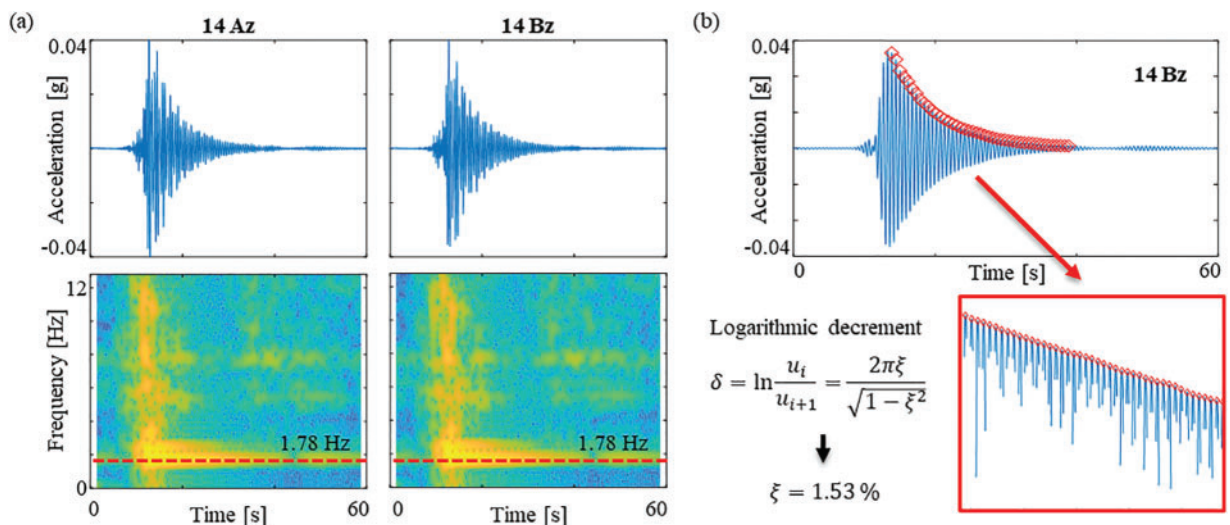


**Figure 11.** Dynamic tests with the truck passages: (a) acceleration recordings and relevant STFTs, (b) damping estimation with the logarithmic decrement method

frequency, were used to calculate damping using the logarithmic decrement method (Fig. 11b). A value equal to 1.53% is obtained, in agreement with the UB damping estimated during AVTs when the bridge was opened to traffic. The parameters estimated from data collected during the truck passage for the DB resulted in values very close to those obtained by the OMA in the case of the bridge closed to traffic. This allowed for comparison and validation of the OMA results while also showing that the passage of a loaded truck did not trigger non-linear phenomena in the structure.

One year later, in April 2023, another experimental campaign was done aiming at investigating the behavior of cracks detected on the half-joints of the UB. During rush hours,

crack openings were measured using a displacement transducer mounted on the side of the deck (details provided in the next section). To correlate crack openings with vehicle passages, a camera was installed over the deck and synchronized with the transducer measurements. In the meantime, the vertical displacements of the UB deck were also measured by using a high-definition camera positioned on the west bank of the river, approximately 50 m far from the deck, and pointing at circular sights installed on the UB deck lateral side. The complete test setup is shown in Fig. 12a. Considering the passage of a heavy truck (truck passage 1 of Fig. 12b) as an example, the relevant time histories of the deck vertical displacements around half-joint one obtained with the high-definition camera are depicted in Fig. 12c.

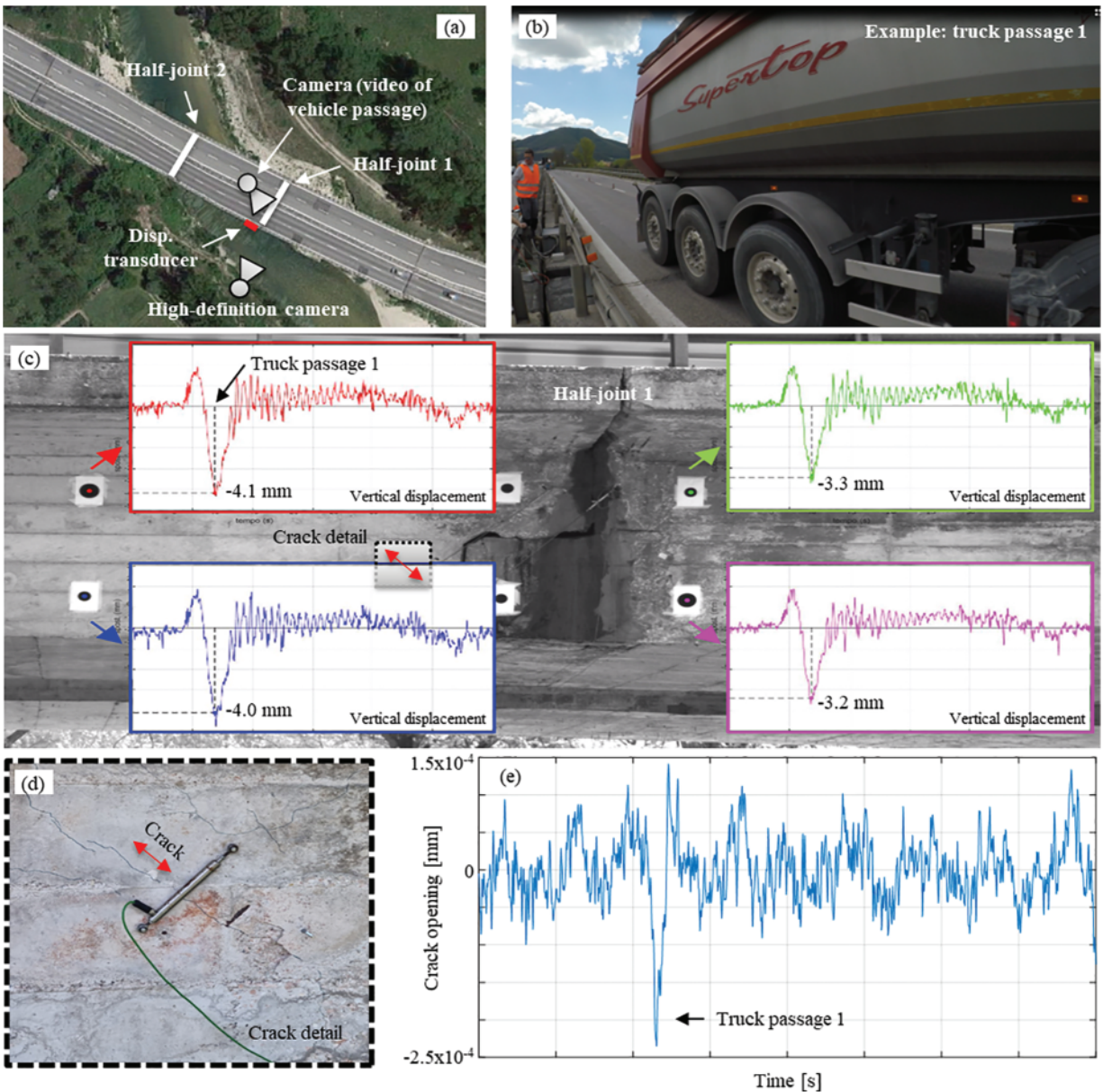


**Figure 12.** Dynamic tests performed in April 2023: (a) measurement setup, (b) example of a heavy truck passage, (c) vertical displacements of targets installed on the lateral side of the deck in correspondence of the half-joint one due to the heavy truck passage, (d) displacement transducer mounted on a diagonal crack close to half-joint one and (e) relevant displacements due to the truck passage

The maximum measured deflection was about 4.1 mm. The vertical displacements observed align with those measured during the static tests conducted in March 2022. However, these static tests do not account for dynamic effects. In the meantime, the opening of the monitored crack was measured as well. Fig. 12d shows the evolution of the crack opening during the test campaign; the peak observed during truck passage 1 was minimal (around  $2.5 \times 10^{-4}$  mm), indicating that the bridge's normal operation, even under heavy loads, did not lead to significant crack openings. This suggests the cracks are unlikely to be caused by regular operating conditions.

Finally, in December 2023, AVTs were repeated on the entire DB bridge to update benchmark data for the final

destructive experimental campaign scheduled for February 2024 before demolition. These tests used the same instrumentation and sensor setup as in March 2022 (Fig. 10a) focusing solely on the DB. Results are reported in Fig. 13. Comparing the modal parameters of the first mode with those obtained in March 2022 (frequency 1.78 vs 1.81 Hz and damping 0.53 vs 0.38%), it is evident that differences are almost negligible and within the variability due to environmental effects. This confirms that the dynamic of the bridge has not changed during the one-and-a-half-year period. Moreover, by observing the modal parameters reported in Fig. 13, it is interesting to note that the first four vibration modes are global modes of the whole bridge, while the 5th, 6th, and 7th modes are a sort of local modes where only some



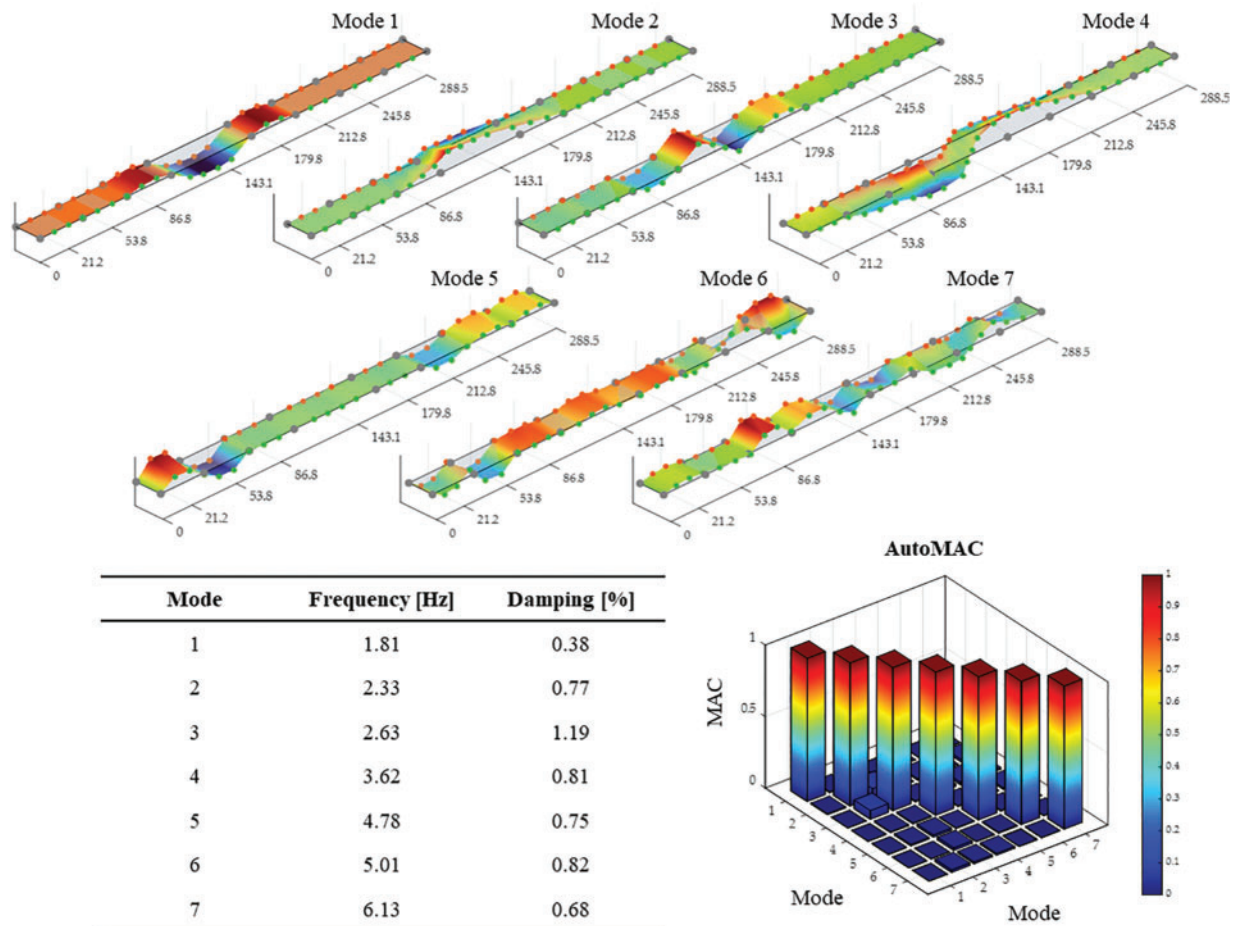


**Figure 13.** Results of the dynamic identification of DB in December 2023

spans are interested. The latter are typical modes of simply supported span bridges.

The correctness of results is also proven by the almost diagonal AutoMAC matrix, which denotes how the identified mode shapes are highly orthogonal to each other. The results of AVTs performed in December 2023 were a key reference point for the analysis of the data collected during the induced damage process of the bridge before its complete demolition. This test campaign was performed in February 2024 and foresaw the progressive damage of prestressing cables of the simply supported span of the Gerber girders. During the induced damage evolution, many static and dynamic tests were performed by different groups coordinated by the FABRE consortium, e.g., AVTs, measurements with high-definition cameras, topographic surveys, measurements of deck deflections with transducers and tiltmeter, etc. However, these tests are still under study, and their outcomes will be disseminated in the future.

### **The continuous SHM of the bridge open to traffic**

In June 2022, the DB was closed to traffic while awaiting demolition and reconstruction; consequently, all the traffic flow was moved to the UB. In conjunction with this decision, the road administrator decided to install an SHM system on the open bridge to guarantee its safety and monitor its use.

The monitoring system is a combined static and dynamic system composed of two 3-axial accelerometers mounted on the east kerb of the cross-section, close to the two half-joints, and 8 Displacement Transducers (DT), mounted in pairs on the two lateral faces of each half-joint. The system is powered by solar panels placed on the DB kerb (Fig. 14).

The accelerometers record the structure vibrations under its operative condition 4 times per day (1 every 6 hours) with a sampling frequency of 100 Hz and time duration of 30 minutes; moreover, the dynamic system is integrated by a trigger that activates the recordings and the data saving whenever excessive accelerations of the deck are detected, for instance due to exceptional natural events (e.g., earthquakes, since the bridge is located in a seismic prone area) or exceptional load conditions (e.g., passage of very heavy loads, collisions, etc.). This trigger is set to measure accelerations with orders of magnitude greater than  $10^{-1}$  g. The displacement transducers are mounted in correspondence with the half-joints to control possible deck crack openings and widenings. They are installed with an extension bar that allows the measurement within 1 m of length to be performed to get the overall value of cracks opening/widening in the section interested by the potential failure mechanisms. These instruments provide one displacement measurement per hour.

The recorded accelerations under the normal use of the structure are processed with AutoOMA techniques to obtain

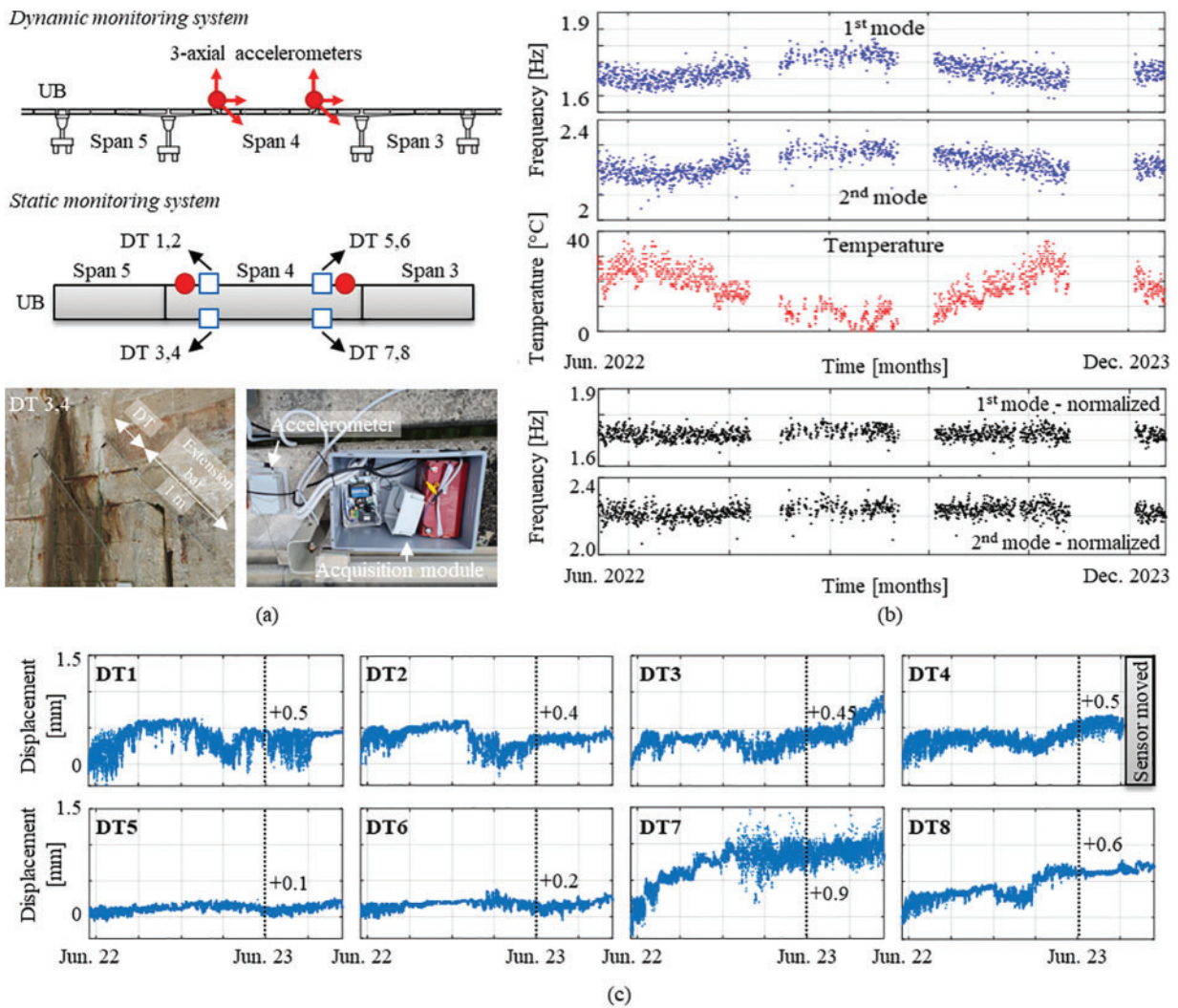


**Figure 14.** Static and dynamic monitoring system: (a) SHM system setup and pictures, (b) dynamic and (c) static monitoring results (+ sign means crack opening/widening)

the modal parameters of the bridge. Given the low number of sensors, only the first modes can be identified without much uncertainty. In Fig. 14b the evolution of the identified resonance frequencies for the first two modes is reported for 1 year and half of monitoring. These modes correspond to the 1<sup>st</sup> and 2<sup>nd</sup> global modes reported in Fig. 13, whose mode shapes mainly involve the Gerber girders. In addition, the evolution of the air temperature for that area is reported as well, the latter obtained from meteorological websites. As can be noted, the resonance frequency evolutions show a cyclical and seasonal fluctuation that is consistent with the temperature variation. Specifically, an inverse trend is clearly evident for both frequencies, namely, when temperature increases, the frequency decreases, and vice versa. For this reason, data normalization is performed, trying to clean temperature fluctuations on frequency data by using a simple mono-parametric linear regression. Results are reported in the bottom part of Fig. 14b. In this case, frequencies show an almost constant evolution around their mean value, and no abrupt changes are evident, thus proving that the bridge experienced no significant damage during monitoring.

Results of the static monitoring are reported in Fig. 14c in terms of displacement time histories. For each transducer, the mean value of measurements after 1 year monitoring (Jun 2022–2023) is reported in the graphs. This data is useful to compare the measurements neglecting the environmental effects on the crack opening/closing. All values are positive, meaning a widening of cracks, albeit very low, being the maximum one lower than 1 mm.

In October 2023, the static monitoring system was slightly modified, moving DT 4 across one crack (thus removing the extension bar) considered worthy of being monitored alone (the same crack monitored during the April 2023 test campaign and showed in Fig. 12d). Also in this case, in this short period of monitoring (Oct.–Dec. 2023), DT 4 experienced a very low widening, about 0.1 mm in 3 months.

## Conclusions

This paper presented a pilot study of the new Italian guidelines from both a scientific and practical standpoint,

providing advanced procedures for the classification, evaluation, and management of existing bridges in line with the philosophy of the innovative Guidelines 2022. The objective is obtained by focusing on two existing prestressed RC box-girder half-joint bridges for which issues related to the visual inspections, safety assessments, experimental testing, and structural monitoring are addressed following prescriptions of the innovative Guidelines 2022. To the authors' best knowledge, this work is one of the first studies in this sense; thus, it offers the first comprehensive discussion in the scientific literature on the application of this multilevel, multi-risk code, proposing, for two prestressed RC box-girder half-joint span bridges adopted as a case study, advanced procedures and considerations for the inspection, safety assessment, testing, and monitoring of the structures. An additional goal is to share such approaches with other researchers and road administrators in the spirit of achieving a best practice for the management of the infrastructure asset and upgrading national standards.

## Acknowledgments

This study was supported by Fabre—"Research consortium for the evaluation and monitoring of bridges, viaducts, and other structures" ([www.consortoziofabre.it](http://www.consortoziofabre.it)) through the project "FABRE-ANAS 2021–2024". Any opinion expressed in the paper does not necessarily reflect the opinion of the funder.

The authors would like to thank ANAS S.p.a., Marche Region division, for the technical support provided and for the helpfulness they demonstrated.

The authors would also like to thank Eng. Chiappini Gianluca who provided support in carrying out the camera surveys and data processing.

## Data Availability Statement

Data, models, or codes that support the findings of this study are available from the corresponding author upon reasonable request.

## Conflicts of Interest

The authors have no competing interests to declare that are relevant to the content of this article.

## References

- [1] Ghafoori M, Abdallah M, Ozbek ME. Machine learning-based bridge maintenance optimization model for maximizing performance within available annual budgets. *J Bridge Eng.* 2024;29(4):4024011. doi:10.1061/JBENF2.BEENG-6436.
- [2] Nagaraju ASV, Kumar R. Effect of climate change on structural safety of RC bridges in coastal region. *Structures.* 2024;63(May):106273. doi:10.1016/j.istruc.2024.106273.
- [3] Dersah SA, Mohammed TA. Bridge structures under progressive collapse: a comprehensive state-of-the-art

review. *Results Eng.* 2023;18(June):101090. doi:10.1016/j.rineng.2023.101090.

- [4] Kalkan Okur E, Okur FY, Altunişik AC, et al. Progressive collapse assessment of osmangazi suspension bridge due to sudden hanger breakage under different loading conditions. *Eng Failure Anal.* 2023;149(July):107269. doi:10.1016/j.engfailanal.2023.107269.
- [5] Valenzuela S, de Solminihac H, Echaveguren T. Proposal of an integrated index for prioritization of bridge maintenance. *J Bridge Eng.* 2010;15(3):337–343. doi:10.1061/(ASCE)BE.1943-5592.0000068.
- [6] Caprili S, Mattei F, Salvatore W. Corrosion effects on the dissipative performance of critical regions of RC frame systems. *Eng Struct.* 2024;300(February):117259. doi:10.1016/j.engstruct.2023.117259.
- [7] Casas JR, Frangopol DM, Turmo J, et al. Bridge safety assessment, maintenance, monitoring, and life-cycle performance. *Struct Infrastruct Eng.* 2024;20(7–8):957–959. doi:10.1080/15732479.2024.2331082.
- [8] MIMS. Decree 17/12/2020, n. 578. Enforcement of the guidelines on risk classification and management, safety assessment and monitoring of existing bridges (Guidelines 2020). In Italian language; n.d.
- [9] MIMS. Decree 1/07/2022, n. 204. Guidelines on risk classification and management, safety assessment and monitoring of existing bridges (Guidelines 2022). In Italian language; n.d.
- [10] ANSFISA. Operative instructions for the application of the guidelines on risk classification and management, safety assessment and monitoring of existing bridges (Guidelines 2022). In Italian language; n.d.
- [11] Natali A, Messina V, Salvatore W, et al. A new tailored developed software for the risk classification of bridges according to the Italian guidelines. *Proc Struct Integr, XIX ANIDIS Conference, Seismic Engineering in Italy.* 2023;44(January):2012–2019. doi:10.1016/j.prostr.2023.01.257.
- [12] Miluccio G, Losanno D, Parisi F, et al. Fragility analysis of existing prestressed concrete bridges under traffic loads according to new Italian guidelines. *Struct Concrete.* 2023;24(1):1053–1069. doi:10.1002/suco.202200158.
- [13] Carbonari S, Nicoletti V, Martini R, et al. Dynamics of bridges during proof load tests and determination of mass-normalized mode shapes from OMA. *Eng Struct.* 2024;310(July):118111. doi:10.1016/j.engstruct.2024.118111.
- [14] Micozzi F, Morici M, Zona A, et al. Vision-based structural monitoring: application to a medium-span post-tensioned concrete bridge under vehicular traffic. *Infrastructures.* 2023;8(10):152. doi:10.3390/infrastructures8100152.
- [15] Santarsiero G, Masi A, Picciano V, et al. The Italian guidelines on risk classification and management of bridges: applications and remarks on large scale risk assessments. *Infrastructures.* 2021;6(8):111. doi:10.3390/infrastructures6080111.
- [16] Natali A, Cosentino A, Morelli F, et al. Multilevel approach for management of existing bridges: critical analysis and application of the Italian guidelines with the new operating instructions. *Infrastructures.* 2023;8(4):70. doi:10.3390/infrastructures8040070.
- [17] Pregnotato M, Giordano PF, Panici D, et al. A comparison of the UK and Italian national risk-based guidelines for assessing hydraulic actions on bridges. *Struct Infrastruct Eng.* 2024;20(1):117–130. doi:10.1080/15732479.2022.2081709.



- [18] Matos JC, Nicoletti V, Kralovanec J, et al. Comparison of condition rating systems for bridges in three European countries. *Appl Sci.* 2023;13(22):12343. doi:10.3390/app132212343.
- [19] Mazzatura I, Natali A, Salvatore W, et al. A methodological proposal for the analysis of bridges inspections data according to the Italian guidelines. *CelPapers.* 2023;6(5):1399–1404. doi:10.1002/cepa.2102.
- [20] Buratti G, Celati S, Cosentino A. The structural risk assessment of existing bridges in Tuscany (Italy) a quick survey-based method. In: Pellegrino C, Faleschini F, Zanini MA, eds. *Proceedings of the 1st Conference of the European Association on Quality Control of Bridges and Structures.* Cham: Springer International Publishing; 2022:845–855. doi:10.1007/978-3-030-91877-4\_96.
- [21] Bencivenga P, Zizi M, Palmieri G, et al. The holistic multi-level approach of recent Italian guidelines applied to the bridges of caserta. *CelPapers.* 2023;6(5):801–807. doi:10.1002/cepa.2192.
- [22] Fattorini F, Salvatore W, Renzi E, et al. Application to the territorial authorities of the “Guidelines for the classification and management of risk, for the evaluation of safety and for the monitoring of existing bridges”. The case study of the Municipality of Rome. *Proc Struct Integr, XIX ANIDIS Conference, Seismic Engineering in Italy.* 2023;44(January):689–696. doi:10.1016/j.prostr.2023.01.090.
- [23] Rossi PP, Spinella N, Recupero A. Experimental application of the Italian guidelines for the risk classification and management and for the safety evaluation of existing bridges. *Structures.* 2023;58(December):105387. doi:10.1016/j.istruc.2023.105387.
- [24] Fox MJ, Furinghetti M, Pavese A. Application of the new Italian assessment guidelines to a, 1960s, prestressed concrete road bridge. *Struct Concrete.* 2023;24(1):583–598. doi:10.1002/suco.202200884.
- [25] Cosenza E, Losanno D. Assessment of existing reinforced-concrete bridges under road-traffic loads according to the new Italian guidelines. *Struct Concrete.* 2021;22(5):2868–2881. doi:10.1002/suco.202100147.
- [26] Miano A, Fiorillo A, Mele A, et al. Risk classification and preliminary safety evaluation for a network of existing RC bridges: an application of the Italian guidelines 2020. In: Aiello MA, Bilotta A, eds. *Proceedings of Italian Concrete Conference 2022.* Cham: Springer Nature Switzerland; 2024:388–398. doi:10.1007/978-3-031-43102-9\_30.
- [27] Sano SD, Costa G, Giordano PF, et al. Multi-risk assessment for bridges: the application of the Italian guidelines. *CelPapers.* 2023;6(5):772–779. doi:10.1002/cepa.2046.
- [28] Miano A, Mele A, Ragione ID, et al. Impact of the structural defects on risk assessment of concrete bridges according to the Italian guidelines 2020. *Infrastructures.* 2023;8(9):135. doi:10.3390/infrastructures8090135.
- [29] Buffarini G, Clemente P, Giovinazzi S, et al. Structural assessment of the pedestrian bridge accessing Civita di Bagnoregio, Italy. *J Civil Struct Health Monit.* 2023;13(8):1499–1516. doi:10.1007/s13349-022-00628-7.
- [30] Consorzio Fabre. April 13, 2024. <https://www.consorziofabre.it/>.
- [31] Palmisano F, Asso R, Chiaia B, et al. Structural assessment of existing R.C. half-joint bridges according to the new Italian guidelines. *J Civil Struct Health Monit.* 2023;13(8):1551–1575. doi:10.1007/s13349-022-00652-7.
- [32] Desnerck P, Lees JM, Morley CT. Impact of the reinforcement layout on the load capacity of reinforced concrete half-joints. *Eng Struct.* 2016;127(November):227–239. doi:10.1016/j.engstruct.2016.08.061.
- [33] NTC2018. Decree 17/01/2018, n. 42. Adjournment of «Technical Code for Constructions», Italian ministry of infrastructures and transports (NTC18). In Italian language; n.d.
- [34] EN 1992-1-1 (2004) (English). Eurocode 2: design of concrete structures-Part 1-1: general rules and rules for buildings [Authority: the European union per regulation 305/2011, directive 98/34/EC, directive 2004/18/EC]; n.d.
- [35] Van Overschee P, Bart DM. Subspace identification for linear systems. Theory, implementation, applications. Incl. 1 Disk. In: *Springer Science & Business Media*, vol. xiv:xiv+254. 1996. doi:10.1007/978-1-4613-0465-4.
- [36] García-Macías E, Ruccolo A, Zanini MA, et al. P3P: a software suite for autonomous SHM of bridge networks. *J Civil Struct Health Monit.* 2023;13(8):1577–1594. doi:10.1007/s13349-022-00653-6.
- [37] Kohm M, Stempniewski L, Stark A. Influence of vehicle traffic on modal-based bridge monitoring. *J Civil Struct Health Monit.* 2023;13(1):219–234. doi:10.1007/s13349-022-00630-z.